Improving Predictability of Renewable Generation through Optimal Battery Sizing

S. Ali Pourmousavi, *Member, IEEE,* P. Wild, and Tapan K. Saha, *Senior Member, IEEE*

***Abstract*—The number of large-scale Photovoltaic (PV) and wind farms is rapidly growing in Australia and all around the world. When these resources participate in the wholesale electricity market, their uncertain nature of generation results in revenue loss due to the penalty incurred by deviating from day-ahead and real-time commitments. In an attempt to avoid financial losses, they typically bid in the market conservatively. This, in turn, might lead to wasting clean energy and lowering overall profit for the producers. To address these issues, various energy storage devices are considered as a potential solution by academic and industrial researchers alike. In this study, an optimal battery sizing methodology is proposed to improve renewable generation predictability using "Seasonal-Trend decomposition based on LOESS[1] (STL)" decomposition technique, self-similarity estimation, and enhancing it through filtering. The ultimate goal is to determine the optimal battery size that enhances predictability of renewable generation regardless of the prediction technique and time horizon, which necessarily improves the accuracy of predicted values. The goal is achieved by the proposed method through designing a forecasting-technique-agnostic algorithm. For optimal battery sizing, an optimisation formulation is proposed including battery degradation through its useful lifetime. Moreover, prediction studies are carried out to prove predictability enhancement using four prediction techniques and three prediction horizons. The simulation results show the effectiveness of the proposed method in improving self-similarity index (i.e., Hurst exponent) in the PV production time series and economic viability of the proposed methodology in a particular application.**

***Index Terms*—Predictability, STL decomposition, self-similarity, optimisation, battery sizing.**

I. Introduction

THE future power system expected to host many utility-scale Photovoltaic (PV) and wind farms, which inevitably demands substantial amount of generation flexibility and storage to compensate their fluctuations, sporadic ramp rates, and lack of inertia. When large-scale renewable generation plants participate in the wholesale electricity market, they are faced with penalty for any deviation from day-ahead and real-time commitment, similar to the conventional generators [1]. Since renewable generation prediction is highly unreliable, they are more likely to be penalised for not fulfilling their commitments [1]. To reduce the risks, renewable plant operators conservatively bids in the market, which consequently reduces their overall profit and wastes a substantial amount of clean energy.

To avoid this, energy storage is considered to compensate forecast uncertainty and alleviate fluctuations in the output power of renewable power plants [1]–[16]. The methods introduced in [1]–[10] used specific forecasting and statistical scenario generation techniques to create different realisation of prediction error. Then, the time series of prediction error is used in different ways to determine the appropriate/optimal battery sizes that can reduce uncertainty of renewable generation prediction. In [1], [2], [4], [5], [8], dynamic battery sizing methods are offered for different trading intervals in the wholesale market based on the statistical behaviour of the forecast error and autocorrelation of the error. These methods are suitable for power system with a separate storage market, where renewable generation can purchase battery capacity dynamically to compensate their deviation from predicted values. In [3], battery sizing and operation algorithms are proposed to maximise distribution companies' profit in the face of day-ahead load/distributed renewable generation uncertainty by following the same concept presented in [1], [2], using the prediction error obtained by a specific forecast method. Other statistical battery sizing methods are proposed in [6], [7], [9], [10], where time series of long-term ([6], [9], [10]) and daily ([7]) forecast error are generated to find an appropriate size of the battery to reduce the error. In [11], different realisations of uncertainty are generated based on a specific forecast method for a set of given battery sizes in an iterative algorithm, which is not scalable nor optimal. The battery sizes obtained by the proposed methods in [1]–[10] might not be optimal for two reasons: first the battery size can vary significantly from one forecasting technique to another, and secondly a single forecast method does not show consistent performance over different prediction horizon and across various parts of a time series [4], [17].

Besides the methods proposed to compensate forecast error, various techniques are developed in [12]–[16] to mitigate fluctuations and smooth output power of the renewable resources. While these methods can improve predictability to some extent, they are not designed to do so, which limits the level of improvement, as it will be shown later in this paper. The battery sizing based on the filtering techniques has two other downsides: first filtering-based approaches in the literature have been applied to the original signal with possibly seasonal and trend components, which makes it difficult to guarantee predictability improvement. Secondly, these approaches require battery to be charged externally, e.g., in [14], which adds to the battery operation cost. In [12], [13], [15], the proposed battery sizing algorithms should be repeated for daily profiles without accounting for the initial state-of-charge (SOC) at the beginning of each day. Also, developing battery sizing methodology based on specific operational strategies and grid codes, e.g., [11], [12], undermines the usability of the proposed methods in other applications. Most of the literature in the field

S. Ali Pourmousavi (a.pour@uq.edu.au) and Tapan K. Saha (saha@itee.uq.edu.au) are with the School of Information Technology and Electrical Engineering (ITEE), and P. Wild (p.wild@uq.edu.au) is with the Global Change Institute (GCI), the University of Queensland, St Lucia, QLD, 4072 Australia.

[1]locally weighted regression

(i.e., smoothing and compensating renewable prediction error) ignored battery capacity degradation over its useful lifetime in the optimal sizing formulation, e.g., [1], [2], [4]–[10], which can play an important role in determining the optimal battery capacity. It is worth mentioning that there are numerous papers on battery sizing for various applications, as summarised in [18]. However, only prior research studies on smoothing and forecast uncertainty compensation are referred in this paper as they are relevant in concept.

In this paper, the battery sizing problem is tackled from a different perspective: by optimally sizing battery storage to improve predictability of the underlying time series without considering a specific forecasting technique. Despite most of the methods presented in [1]–[16], the proposed battery sizing strategy in this paper does not require any type of forecasting technique. Rather, it uses the time-series predictability concept from self-similarity theory to reshape a time series in a way that enhances its prediction. This will, in turn, result in prediction improvement regardless of the forecast horizon because of modifying the original time series without being dependant on a specific forecast method, as shown in the simulation results in Section III-E. To do so, the concept of seasonal decomposition, self-similarity enhancement of a time series, and a filtering technique are applied in the proposed sizing algorithm. First, procedures are developed to identify seasonality and trend in the PV production time series. It is then followed by introducing Seasonal-Trend decomposition based on LOESS[2] (STL) as a sophisticated seasonal decomposition technique [19]. The outcome of STL would be an energy-neutral charge and discharge profile of the battery, which dismisses external charging of the battery from the grid. Then, a procedure is developed to verify the stationarity of the irregular stochastic component through appropriate statistical tests. Then, self-similarity estimation is conducted on the stationary time series using Hurst exponent [20], which is extensively used in other research areas such as stock markets [21] and biomedical engineering [22] for predictability measurement. Since there is no analytical quantitative relationship between Hurst exponent and the prediction accuracy, we developed a strategy to find optimal battery sizes that can improve forecast accuracy in Subsection II-D, where a nonlinear optimisation problem is formulated. The battery capacity degradation throughout its useful lifetime is also formulated in the battery sizing problem. In [23], a nonlinear battery degradation is integrated with the battery/ultra-capacitor sizing formulation, and is solved by DIRECT search method. Whereas, the linear degradation model of this paper preserves linearity of the original optimisation problem, which can be readily solved with gradient-based exact methods. Battery degradation is also used in [24] in a Markov model-based battery sizing study, where the transition probability between states are modified to account for the battery capacity ageing. The proposed method, however, does not guarantee optimality of the solutions nor does offer an optimal formulation for such application. Additionally, the battery charge and discharge efficiencies are accurately modelled, despite studies such as [11]. The contributions of the paper can be summarised as follow:

- Hypothesising, formulating and solving battery sizing problem as a mechanism to improve predictability of renewable generation through converted bi-level programming to tractable nonlinear optimisation problem;
- Application of STL decomposition technique and Hurst exponent of self-similarity theory in the context of power system, which resulted in: 1) avoiding external battery charging and consequently operation cost reduction, and 2) a forecasting-technique-agnostic method for battery sizing in prediction uncertainty mitigation and smoothing applications;
- Adding battery degradation over its useful lifetime in the optimisation formulation as a linear constraint in the battery SOC calculation.

To show the effectiveness of the developed methodology, it is applied to the PV generation data, without loss of generality, gathered from 3.275 MWp PV plant located at the University of Queensland (UQ), Gatton campus, Australia. It is shown that the Hurst exponent of the time series, and consequently predictability, is improved with appropriate size of battery. To further verify forecasting improvement and accuracy of Hurst exponent estimation, four prediction methods are developed to perform a preliminary forecasting study. Finally, a simple economic viability assessment, including battery capacity degradation throughout its lifetime, is carried out to show that there are economic incentives to use battery for prediction improvement in order to avoid paying for the balancing services in the wholesale market. The proposed method is applicable to other variable renewable generation (such as wind) without any alterations in the proposed method as long as the underlying time series is (or can become) trend- and seasonal-stationary and a self-similar process.

The rest of the paper is organised as follows: Section II explains the proposed method step-by-step. Linear and nonlinear battery optimal sizing formulations are described in this section. Simulation studies are carried out in Section III, and the results are explained in detail. Finally, paper is concluded in Section IV.

II. Proposed Methodology

Despite all the improvement in prediction techniques, renewable generation (such as PV) forecast contains large errors particularly for longer horizons [25], [26]. This might lead to revenue loss for the plant operators by conservatively bidding in the market and being penalised for not meeting predicted values. As a result, improving predictability of the renewable generation using storage devices within a plant could be technically and economically beneficial for every stakeholder.

Predictability is a measurable feature in a time series; in fact, it can be defined independently without relying on any specific type of prediction method. One category of predictability measurement approaches is developed based on the theory of long-term self-similarity or long-memory of a time series, which has been expanded by the fractal analysis of time series [27]. In this theory, predictability of a time series is quantified by estimating Hurst exponent. As it is shown in

[2]locally weighted regression

[28], higher Hurst exponent results in lower prediction error of the underlying time series. In this study, a new battery sizing method is developed based on improving self-similarity using Hurst exponent for a stationary time series, as shown in Fig. 1. In the following subsections, every step of the proposed method is explained in detail.

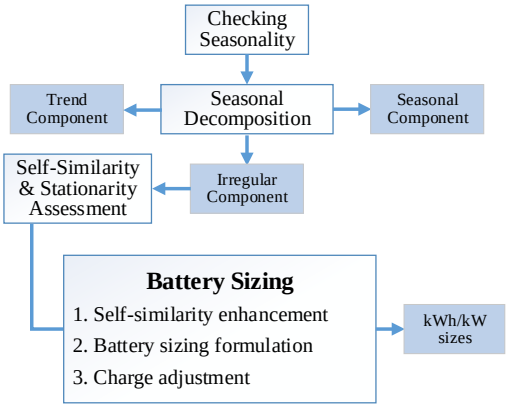

Fig. 1. A step-by-step schematic of the proposed battery sizing methodology

A. Checking Seasonality Existence

The first step is to check the existence of seasonality in the original data. This is necessary because self-similar processes are only defined for stationary time series [27]. Therefore, existence of seasonal and/or trend components in the time series should be identified and effectively removed from the time series beforehand. In this context, seasonality is defined as a regular pattern of fluctuations in a time series that repeats every s time periods, where s specifies the length of the time in which pattern duplicates itself. More explanations about the seasonality and decomposition is presented in Subsection II-B. To check the existence of seasonality in a dataset, multiple visual methods can be used [29]. In this study, autocorrelation function (ACF) plot is preferred as it works well when the seasonal period is unknown.

Let the time series be denoted by z_t,$t \in \mathcal{T}$ where observations made at equidistant time intervals $\mathcal{T} = \{\tau_0 + \mathbf{h}, \tau_0 + 2\mathbf{h}, \ldots, \tau_0 + t \cdot \mathbf{h}, \ldots, \tau_0 + N \cdot \mathbf{h}\}$. The autocorrelation at lag k can be calculated as follows [30]:

$$\rho_k = \frac{\mathbb{E}[(z_t - \mu)(z_{t+k} - \mu)]}{\sqrt{\mathbb{E}[(z_t - \mu)^2].\mathbb{E}[(z_{t+k} - \mu)^2]}} \tag{1}$$

where μ is the average of the entire set; and $\mathbb{E}$ is the expected value operator. The ACF is then calculated for different k using Eq. (1). The time period of seasonality, s, can be easily identified from the ACF graph. The application of ACF is based on the fact that a random process with an underlying trend shows autocorrelation to some extent. In principle, if ACF has a very long (or mathematically infinite) decay rate, the time series represents a Gaussian process, which sometimes is called long-memory process [29]. It means that some processes (such as PV generation time series), while seems to be purely white noise, might exhibit statistical behaviour of long-memory processes. We will use this property of time series in Subsections II-C and II-D along with self-similarity of stochastic processes to develop a battery sizing methodology.

B. Seasonal Decomposition

When seasonality existence is verified and its time period s is identified, seasonality can be removed from the samples. This process is called "Seasonal Decomposition." Typically, every seasonal decomposition algorithm categorises underlying time series z_t as a function of its trend, seasonal, and irregular components. "Additive" and "multiplicative" decomposition methods are two functional forms that relates different components of the seasonality together. In this study, additive model is preferred because the seasonal fluctuation is comparably constant over time:

$$z_t = T_t + S_t + I_t \tag{2}$$

where T_t is the deterministic and non-seasonal trend component; S_t is the deterministic seasonal component with known period s; and I_t is the stochastic irregular component. Various techniques are proposed for seasonal decomposition [31]. In this study, STL decomposition technique is preferred because of its versatility and robustness [31]. The STL technique is explained in detail in [19], and summarised in Algorithm 1. Except for z_t, which is the underlying time series, appropriate methods are offered in [19] to select input parameters in Algorithm 1.

Algorithm 1 Additive STL Decomposition Technique

Input Parameters: $z_t, v, n_o, n_i, s_w, s_d, t_w, t_d, l_w, l_d$
$\mathcal{T}_v^{(0)} \leftarrow 0$, $\rho_v^{(0)} \leftarrow 0$
for $i \leftarrow 1, n_o$ **do**
  for $j \leftarrow 1, n_i$ **do**
    STEP 1: DE-TRENDING
      $\gamma_t^{(j)} \leftarrow z_t - T_t^{(j)}$
    STEP 2: CYCLE-SUBSERIES SMOOTHING
      $\mathcal{C}_v^{(j)} \leftarrow$ LOESS (s_w, s_d) on $\gamma_t^{(j)}$
      Extend smoothed values 1 sample to the right and left
    STEP 3: LOW-PASS FILTERING
      $\mathcal{L}_v^{(j)} \leftarrow$ Twice Moving-Average of length v
      $\mathcal{L}_v^{(j)} \leftarrow$ Moving-Average of length 3
      $\mathcal{L}_v^{(j)} \leftarrow$ LOESS (l_w, l_d)
    STEP 4: DE-TRENDING
      $\mathcal{S}_v^{(j)} \leftarrow \mathcal{C}_v^{(j)} - \mathcal{L}_v^{(j)}$
    STEP 5: DE-SEASONALISATION
      $\gamma_v^{(j)} \leftarrow z_t - \mathcal{S}_v^{(j)}$
    STEP 6: TREND SMOOTHING
      $\mathcal{T}_v^{(j)} \leftarrow$ LOESS (t_w, t_d) on $\gamma_v^{(j)}$
  end for
  $\mathcal{R}_v^{(i)} \leftarrow z_v - \mathcal{S}_v^{(i)} - \mathcal{T}_v^{(i)}$
  $h \leftarrow 6 \times$ median $\left(|\mathcal{R}_v^{(i)}|\right)$
  $\rho_v^{(i)} \leftarrow \mathcal{B}\left(\frac{|\mathcal{R}_v^{(i)}|}{h}\right)$ ▷ $\mathcal{B}$: bi-square weight function
end for

C. Self-Similarity and Stationarity Assessment

In the previous sub-section, it was mentioned that the first two components are deterministic, which can be modelled (or predicted) accurately [31]. The irregular component, however, is difficult to model and predict because it contains most of

uncertainty in the original time series. Therefore, any effort to improve predictability of the time series should be focused on the irregular stochastic component, i.e., I_t. In other words, optimal battery sizing study only requires samples from the irregular stochastic component.

In general, self-similarity is the key property to improve the accuracy of prediction [28]. A stochastic process, denoted by I_t,$t \in \mathcal{T}$, is self-similar with self-similarity exponent of H if for all $c > 0$, the processes of $I_{c.t}$,$t \in \mathcal{T}$ and $c^H.I_t$,$t \in \mathcal{T}$ have the same finite-dimensional distributions [20]. In other words, if I_t,$t \in \mathcal{T}$ is a wide-sense stationary process, then its self-similarity can be measured by Hurst exponent $0 < H < 1$ [20], [28], [32]. For self-similar processes, Hurst exponent varies between $0.5 < H < 1$.

To verify the stationarity of a uni-variate time series, which is the pre-requisite condition prior to Hurst exponent estimation, Augmented Dickey-Fuller (ADF) and Kwiatkowski-Phillips-Schmidt-Shin (KPSS) tests can be utilised [28]. The ADF examines the null hypothesis of a unit root [33], while the KPSS test determines if a time series is stationary around a mean or linear trend [34]. In the latter, the null hypothesis of a uni-variate time series is trend-stationary against the alternative hypothesis that the time series is non-stationary unit root process. When ADF test rejects existence of a unit root (i.e., rejecting null hypothesis) and KPSS test does not reject the trend-stationarity of the time series (i.e., not rejecting null hypothesis), they collectively imply that the underlying process is stationary.

When it is proved that the underlying stochastic process is stationary, self-similarity of the time series can be properly evaluated by the Hurst exponent. The conventional Hurst exponent estimation techniques evaluate time series as a whole to provide a single exponent value characterising the global behaviour of the time series. A comprehensive list of nine methods for Hurst estimation is tested in [35], where the "Aggregated Variance Method" found to be the most reliable technique, although it does not guarantee the best performance for any time series. In this paper, three methods, i.e., "Aggregated Variance Method", "R/S Analysis" and "Average Wavelet Coefficient", are used to estimate Hurst exponent of different time series of interest.

D. Battery Sizing

The optimal battery sizes for predictability improvement of a given renewable generation profile is the trade-off between the cost of the battery and the benefits obtained by the battery operation. Assuming a negligible O&M cost for modern battery technologies (such as Li-based batteries), the capital cost of the devices can be estimated considering its ageing over lifetime, as discussed in Subsection III-F. However, estimating the benefits of the battery operation in this application is fairly complicated. In fact, there are four different sources of benefits that can be obtained from the battery operation, where the first three sources of income are directly related to the amount of predictability enhancement:

- Higher energy sold in the energy/capacity market due to higher confidence in predicted values (i.e., maintaining the headroom at a lower level);
- Avoiding/lowering penalty paid to the balancing market because of reduction in forecast errors;
- Opportunities to earn money in the balancing market by offering services such as down regulation; and
- Since battery will not be operating to improve predictability at the full energy/power capacity most of the time, it can be used to deliver other services (e.g., reactive power/voltage support) to create new revenue streams, which is known as stack application. Although it is not directly related to the predictability improvement, it can be considered as a source of income for the battery in such applications to recover the incurred costs.

Estimating the direct benefits of the battery in this framework is not trivial because it depends on the improvement in the accuracy of the predicted values (for the first three sources of benefits mentioned above). In one hand, the irregular stochastic component, I_t, contains most of the uncertainties in the original signal; hence, it is less predictable, as it is shown in Subsection III-E. On the other hand, a quantitative relationship between predictability of a time series with the actual improvement in prediction does not exist to estimate the true benefits of battery operation. To bypass this issue, we developed a strategy that is shown in Fig. 2, where a filtering technique is used to separate less predictable components, i.e., $\hat{I}_t$, from more predictable ones, i.e., $\overline{I}_t$, in the irregular stochastic signal, as explained in Subsection II-D1. Then, an optimisation formulation is developed in Subsection II-D2 to find the optimal battery size for the less predictable components, $\hat{I}_t$. To show the improvement of predicted values, a comprehensive forecast study is carried out in Subsection III-E with multiple prediction techniques and horizons. Finally, a standard economic viability analysis is performed for different battery sizes in Subsection III-F to assess the economic consequences of the proposed solution.

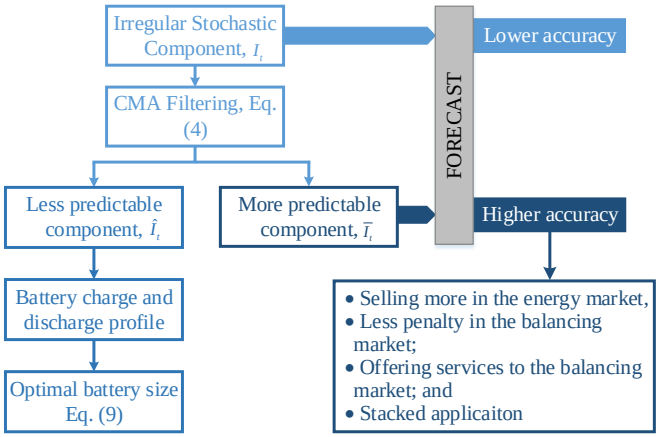

Fig. 2. Battery sizing problem definition in this study

1) Self-Similarity Enhancement: To improve the predictability (i.e., self-similarity) of the irregular stochastic component, which leads to more accurate prediction of the underlying time series, one option is to find the minimum size of the battery that can cover the entire irregular component obtained from the seasonal decomposition. This, however, might lead to oversized battery, as it will be shown in the simulation results.

To avoid this, a part of the irregular stochastic time series can be selected for battery sizing study, while improving self-similarity of the smoothed signal. In this study, causal moving average (CMA) filter with equal weights is used, where the residual of the filter is utilised in the battery sizing study. This way, smoothed output of the filter, $\overline{I}_t$, is the part remaining to be predicted, and the residual values, $\hat{I}_t$, are covered by the battery.

$$\hat{I}_t = I_t - \overline{I}_t \tag{3}$$

In its simplest form, a CMA filter of length ω takes the average of every ω consecutive samples of the waveform from the past. The first-order CMA of length ω for I_t,$t \in \mathcal{T}$ can be calculated as follows:

$$\overline{I}_t = \frac{1}{\omega} \sum_{i=t-\omega+1}^{t} I_t, \quad \omega \leq t \leq N \tag{4}$$

where ω is the window length; and $\overline{I}_t$ is the smoothed signal. It is known that the larger the moving average window, the more the lag. To check on the impact of filtering delay on the battery sizes [14], Savitzky-Golay (S-Golay) filter, known to be lag free and preserving high frequency component, is also tried [36], the outcome of which is briefly discussed in the simulation results.

2)Battery Sizing Formulation: In order to find minimum size of the battery to cover $\hat{I}_t$, the following optimisation problem should be solved over the entire training dataset:

$$\min \quad E + \lambda \cdot SOC_0 \tag{5a}$$

s.t.

$$\underline{\mathbf{SOC}} \cdot E \cdot \alpha_t \leq SOC_t \leq \overline{\mathbf{SOC}} \cdot E \cdot \alpha_t \quad \forall t \in \mathcal{T}, \tag{5b}$$

$$\underline{\mathbf{SOC}} \cdot E \leq SOC_0 \leq \overline{\mathbf{SOC}} \cdot E, \tag{5c}$$

$$SOC_t = SOC_0 + \eta^{(.)} \sum_{j=1}^{t} \hat{I}_j^{(.)} \cdot \mathbf{h} \quad \forall t \in \mathcal{T}, \tag{5d}$$

$$E, SOC_0 \geq 0 \tag{5e}$$

where E is the optimal capacity of the battery in kWh; SOC_0 is the initial capacity of the battery and a decision variable in kWh; λ is the penalty coefficient for initial battery SOC to make it as small as possible ($\lambda = 10^{-6}$); $\underline{\mathbf{SOC}}$ and $\overline{\mathbf{SOC}}$ are normalised lower and upper SOC of the battery; $\eta^{(.)}$ is the normalised charge and discharge efficiency of the battery; and $\mathbf{h}$ is the sampling time in hour. Positive values of $\hat{I}_t^{(.)}$ represent charging while negative values show battery in discharging mode. Having the initial battery SOC, i.e., SOC_0, in the optimisation formulation avoids the negative impact of arbitrary SOC_0 on the battery optimal size and initial cost. The goal is to minimise the battery kWh size while minimising the initial SOC of the battery as a penalty factor. In this formulation, battery power is multiplied by $\eta_d > 1$ during discharge mode to correctly represent battery inefficiency. α_t is the linear battery capacity degradation over its useful lifetime, and calculated by:

$$\alpha_t = 1 + (\text{EOL} - 1) \cdot \frac{\mathcal{C}_t}{\mathcal{C}_{\text{total}}} \tag{6}$$

where EOL is the end-of-life (EOL) of the battery in p.u. (0.65 in utility-scale storage application); $\mathcal{C}_t$ is the energy throughput of the battery until time t in kWh; and $\mathcal{C}_{\text{total}}$ is the rated energy throughput during its entire useful lifetime. The last two terms can be calculated by:

$$\mathcal{C}_t = \eta^{(.)} \sum_{j=1}^{t} |\hat{I}_j^{(.)}| \cdot \mathbf{h} \tag{7a}$$

$$\mathcal{C}_{\text{total}} = 2 \times \text{DoD}_\text{r} \cdot \frac{\eta_c}{\eta_d} \cdot E \cdot \sum_{j=0}^{\mathbf{N_r}} \left(1 + \frac{\text{EOL} - 1}{\mathbf{N_r}} \cdot j\right) \tag{7b}$$

where DoD_r is the rated depth-of-discharge; and $\mathbf{N_r}$ is the rated battery cycles. The power size of the battery, i.e., $\mathbf{P_{max}}$ is the maximum absolute power of $\hat{I}_t$ time series, which can be determined prior to optimisation:

$$\mathbf{P_{max}} = \max |\hat{I}_t| \tag{8}$$

3)Charging Adjustment: The CMA residual, i.e., $\hat{I}_t$, is energy neutral over the entire samples. It follows the theory of seasonal decomposition, where stochastic component will have zero mean [37]. In addition, it is shown in different literature that charging is less efficient than discharging in Li-Ion batteries partially due to different efficiency of inverters during charging and discharging modes [38]. Considering battery charge (η^c) and discharge (η^d) efficiency as well as the energy neutrality, it implies a systematic energy deficit in the battery to fulfil discharge requirements. It will be problematic in the battery sizing study (i.e., Eqs. (5a)-(5e)) because the energy deficit will be compensated by over-sizing the battery in order to take advantage of its initial SOC. It also raises technical issues regarding battery self-discharge as it becomes more prominent in such cases. To resolve this issue, charging adjustment factor (i.e., δP_c) is defined to shift the stochastic component upward to compensate the difference between charge and discharge inefficiencies. Although δP_c is intentionally kept small to avoid jeopardising the stationarity of the irregular pattern, it has a significant effect on the battery kWh size, which will be shown in the simulation results. Therefore, it is important to find optimal value of δP_c by solving an optimisation problem, as follows:

$$\min \quad \delta P_c, E + \lambda \cdot SOC_0 \tag{9a}$$

$$s.t: \quad \min \left\{ \begin{array}{c} E + \lambda \cdot SOC_0 \\ s.t: \\ 0 \leq \hat{I} + \delta P_c \cdot \hat{I}_{\text{diff}} \leq \mathbf{P_{max}}, \\ \underline{\mathbf{SOC}} \cdot E \cdot \alpha_t \leq SOC_t \leq \overline{\mathbf{SOC}} \cdot E \cdot \alpha_t, \\ \underline{\mathbf{SOC}} \cdot E \leq SOC_t \leq \overline{\mathbf{SOC}} \cdot E, \\ SOC_t = SOC_0 \\ \quad + \eta^{(.)} \sum_{j=1}^{t} \left(\hat{I}_j^{(.)} + \delta P_c \cdot \hat{I}_{\text{diff}}\right) \\ \quad \times \mathbf{h} \\ E, SOC_0 \geq 0 \end{array} \right\}, \tag{9b}$$

$$0 < \delta P_c \leq \overline{\delta P_c} \tag{9c}$$

where $\hat{I}_{\text{diff}}$ is the difference between maximum and minimum value over the entire samples in $\hat{I}_t$. Equation. (9b) is the original optimisation formulation in Eqs. (5a)-(5e), which is modified to account for δP_c. Despite the original optimisation problem in Eqs. (5a)-(5e), the optimisation formulation in Eq. (9b) is non-linear because δP_c is changing by the upper optimisation problem. The nature of the formulation suggests a multi-objective bi-level programming [39]. However, it is very difficult, if possible at all, to solve such a non-linear bi-level problem. Therefore, the bi-level formulation is replaced by an intuitive substitute, where the upper-level problem only minimises δP_c in the objective function while minimising the lower-level problem as a constraint. Therefore, a single-level non-linear optimisation can be solved.

To verify the accuracy of the non-linear optimisation results, an exhaustive search is implemented to find the optimal value of δP_c. In the first step, N equidistant numbers are generated within the given limits in Eq. (9c) for a given $\overline{\delta P_c}$. Then, the optimisation problem in Eqs. (5a)-(5e) is solved for each δP_c value, and the minimum size of the battery is identified based on the optimisation results. Afterwards, the upper and lower limits of δP_c is updated in Eq. (9c). The loop is continued until the difference of the present and previous minimum battery size becomes less than a given threshold. In the simulation study, the results of exhaustive search are compared with those obtained by solving non-linear optimisation problem.

III. Simulation Study

To show the applicability of the proposed approach, a simulation study is carried out with actual minute-by-minute PV generation data, collected from a 3.275 MWp PV plant located at the UQ Gatton campus. Details about the plant specification and operation can be found in [40] and [41]. The data used in this study are collected from 1$^{\text{st}}$ of June 2015 to 17$^{\text{th}}$ of January 2018. 90% of the daily profiles from the beginning are selected for optimal battery sizing study, i.e., training dataset, and the remaining 10% of data, i.e., test dataset, is used to evaluate the effectiveness of the proposed approach in terms of maximum and minimum SOC levels, charge and discharge power, and prediction improvement.

A. Checking Seasonality

In this subsection, seasonality existence is examined based on the procedure introduced in Subsection II-A. The ACF for the training samples is plotted in Fig. 3 for up to 30 days lag. Distinct cyclic behaviour can be identified from the ACF graph. The same behaviour is observed for the testing dataset. The distance between peaks, which represents periodicity s, is almost a complete day (i.e., $s = [1434, 1445]$ minutes). In addition, the trend existence can be confirmed by the slow decay rate of the peaks, as shown in Fig. 3.

B. Seasonal Decomposition

Since there is an obvious periodicity in the time series, it should be decomposed into trend, seasonal, and irregular stochastic components, as explained in Subsection II-B. The STL algorithm is developed in MATLAB® for this study. The parameters of the STL decomposition are reported in Table I. Seasonal decomposition is carried out for the entire data (i.e., training and testing datasets) as irregular stochastic component is needed for the sizing and prediction studies.

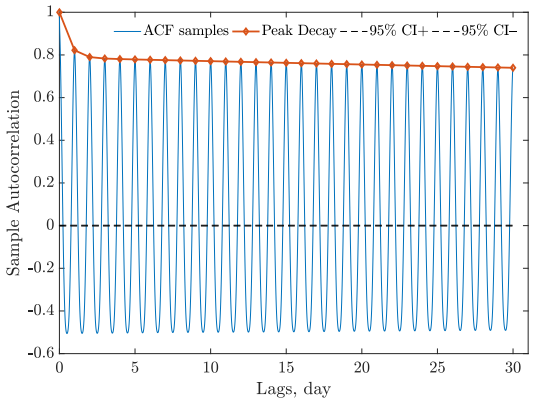

Fig. 3. The ACF plot of the training dataset

TABLE I
STL PARAMETERS FOR SEASONAL DECOMPOSITION

Parameter	v	n_o	n_i	s_w	s_d	t_w	t_d	l_w	l_d
Value	1440	2	3	2401	0	1441	1	2162	1

In Fig. 4, the three components extracted from the original time series are plotted against the original data. The periodicity of the seasonal component is clear from the zoomed-in part of Fig. 4(b). It also can be seen that the stochastic residual is shifted downward with an average around zero, as expected by the theory. According to [31], the trend component of the STL decomposition (shown in Fig. 4(a)) is nonlinear and nonparametric. However, the uncertainty in this component is much smaller than the irregular pattern; hence more predictable.

C. Self-Similarity and Stationarity Assessment

To prove the stationarity of the irregular signal, the ADF and KPSS tests from Subsection II-C are performed on the training and test samples separately. The null hypothesis in the ADF test is rejected by p-value of 0.001 (for 95% confidence interval), where the ADF stat value of -172.2 was significantly lower than the critical value of -1.94. The KPSS test result indicates that the test fails to reject the null hypothesis, where p-value, test stat, and "test critical value" are 0.1, 0.018, and 0.463, respectively. Therefore, the stochastic component, in this example, is a stationary time series. The Hurst exponent is also estimated for the irregular stochastic component at about 0.666, 0.508, and 0.819 calculated by "Aggregated Variance Method", "R/S Analysis", and "Average Wavelet Coefficient" method, respectively. While the Hurst exponents are different for various approaches, they are within 0.5 and 1 range, which verifies the self-similarity of the underlying signal.

D. Battery Sizing

The parameters of the simulation studies are $\eta^c = 0.9$; $\eta^d = \frac{1}{0.93}$; $\underline{\mathbf{SOC}} = 0.2$; and $\overline{\mathbf{SOC}} = 1.0$, and only training data is used for battery sizing.

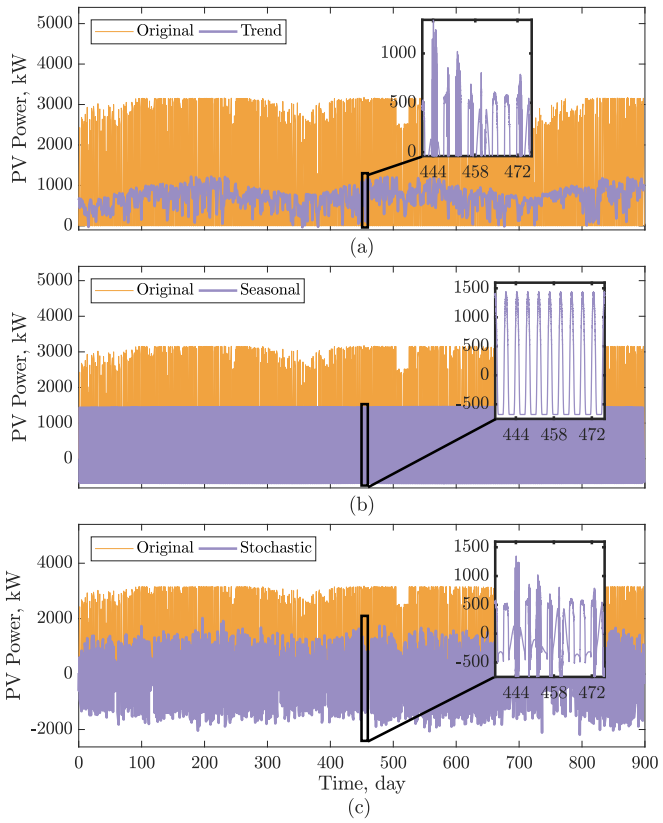

Fig. 4. Seasonality decomposition of the PV time series: (a) original vs. trend, (b) original vs. seasonal, and (c) original vs. irregular stochastic

1)Self-Similarity Enhancement: An CMA filter is offered in Subsection II-D1 to improve self-similarity/predictability of the irregular stochastic time series. Different arbitrary length of averaging window is tried in this study, i.e., $\omega \in \{216, 288, 360, 432\}$ minutes. The Hurst exponents of the new irregular stochastic time series (i.e., the smoothed signal in the output of the CMA filter) are reported in Table. II, calculated by three methods. It can be seen that the self-similarity of the irregular time series has been improved substantially in all cases compared to the unfiltered irregular component. Moreover, it shows that longer CMA window results in larger improvement in the Hurst exponent.

TABLE II
HURST EXPONENT OF FILTERED SIGNALS: NO CHARGING ADJUSTMENT

ω, minute	216	288	360	432
Aggregated Variance Method	0.732	0.742	0.752	0.760
R/S Analysis	0.521	0.569	0.603	0.627
Average Wavelet Coefficient	0.861	0.899	0.926	0.945

2)Battery Sizing without Charging Adjustment: To find the optimal battery sizes without charging adjustment, optimisation problem in Eqs. (5a)-(5e) is solved for the residual time series from previous sub-section. Gurobi® solver [42] is used in MATLAB® to obtain optimal kWh sizes. The optimal power of the battery is also calculated by Eq. (8).

Optimal battery sizes for smoothed time series are reported in Table III. The power size of the battery is almost the same

TABLE III
BATTERY SIZES FOR DIFFERENT CMA FILTER: NO CHARGE ADJUSTMENT

ω, minute	216	288	360	432
Energy, MWh	468.38	526.03	573.44	612.33
Power, MW	2.58	2.63	2.63	2.58

for all cases. However, the bigger the CMA window, the larger the battery capacity. The kWh size in all cases is unusually large because of the issue explained in Subsection II-D3. The required capacity to cover the entire irregular component without filtering, i.e., I_t, is as high as 1,757,834.3 MWh, which is technically and economically an impossible solution. Therefore, there is a trade-off that should be made between the predictability enhancement and battery size, which is offered in this paper by using CMA filter.

3)Battery Sizing with Charging Adjustment: In this section, non-linear optimisation problem, i.e., Eq. (9), is solved to adjust charging profile while minimising battery capacity. The optimisation problem is solved in MATLAB® using `fmincon` non-linear optimisation solver and "sequential quadratic programming" technique. The results of the battery sizing along with the optimal δP_c values are given in Table IV. It can be seen that the MWh sizes of the battery reduced substantially (at least 20.8 times) in comparison with the optimal sizes without charging adjustment in Table III. It is achieved by slightly shifting smoothed time series upward (less than 26 kW) so that the accumulated charged energy is slightly bigger than discharge. This is achieved while the Hurst exponents of the shifted smoothed time series are identical to those without charging adjustment (reported in Table II).

TABLE IV
BATTERY SIZES FOR DIFFERENT FILTERS: CHARGE-ADJUSTED PROFILE

ω, minute	216	288	360	432
Energy, MWh	22.46	24.80	26.88	28.87
Power, MW	2.60	2.65	2.66	2.60
Optimal δP_c, kW	20.03	22.41	24.35	25.95

In order to verify the accuracy of the non-linear optimisation, exhaustive search has also been implemented to find optimal δP_c, as shown in Fig. 5. The green markers are the results of exhaustive search with $N = 10$, battery size tolerance of 50 kW, and $\delta P_c \in [0, 0.02]$ p.u. The red squares in Fig. 5 are the results obtained by the non-linear optimisation. For the four ω values, it can be seen that the exhaustive search results are converged to the optimal values obtained by the non-linear optimisation. From the figure, the sensitivity of the battery energy size to the δP_c can be noticed, which shows the importance of calculating optimal δP_c. The exhaustive search was about 12 times slower on average compared to the non-linear optimisation problem. Employing the S-Golay filter increased battery kWh sizes for about 1.7% while reducing the Hurst exponent for 3.6∼4.8% with the same filter length. Therefore, application of the CMA filter is more suitable for the data of this study.

To ensure that the optimal battery sizes are legitimate for the test data, battery SOC is calculated and charge and discharge

power are compared against the optimal values. For the entire test dataset, there were 3 charging and 1 discharging power violations (among 128160 observations from 88 test days) for ω_1 filter, while no power violations have occurred in other filters. The maximum charging and discharging violations in ω_1 were 24.7 kW and 61.9 kW, respectively. The upper and lower SOC violation never occurred for the given filters.

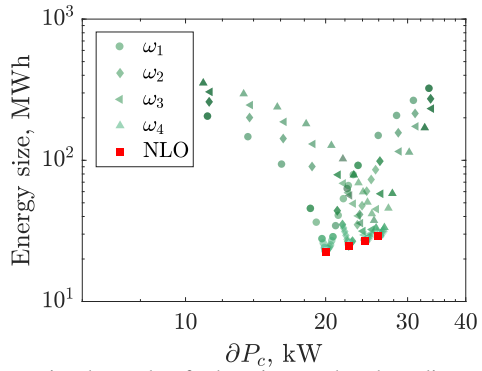

Fig. 5. Comparing the results of exhaustive search and non-linear optimisation on logarithmic axes: Exhaustive search converged in 9, 8, 10, and 10 iterations for ω_1, ω_2, ω_3, and ω_4, respectively. Different colour intensity of the same marker represents different iteration.

E. Prediction Study and Comparison

In order to verify the prediction accuracy improvement after self-similarity enhancement, forecasting studies are carried out using four different prediction techniques, namely *naïve*, *random-walk*, *Markov Chain*, and *Artificial Neural Network (ANN)* models.

- ◇ In *naïve* method, the mean of previously observed samples (200 samples in this study) are used for prediction [17].
- ◇ *Random-walk* method uses the previous observations as the forecast [17]. In some texts, it is called persistent method.
- ◇ *Markov Chain* can be used as a stochastic method for non-linear time series prediction [43]. When the state vector is known, transition probability matrix (TPM) can be formed using historical data, which later can be used to predict the next value in line, as explained in [44]. In this study, 50 days worth of data from the past is used to create TPM, and the number of states was 200.
- ◇ *ANN* is a well-known machine learning tool that is frequently used to model complicated and nonlinear relationships among any number of input and output parameters. Various models of ANN have been used in numerous forecasting studies in literature, e.g., [45]. In this study, multi-layer perceptron feedforward ANN is used with 50 days of minute-by-minute data for training the network using Levenberg-Marquardt algorithm. In this paper, the ANN model is constructed by 100 inputs parameters (100 immediate datapoints before the prediction time), one output (1-minute ahead predicted value), and 1 hidden layer with 5 neurons.

Prediction studies are performed for test dataset in 1-step, 5-step, and 60-step ahead using the optimal battery sizes obtained in previous subsection. 5- and 60-step ahead forecasts generated recursively: i.e., train the model using the existing data from previous day, use that model to perform a one-step ahead prediction, iterate one-step prediction using predicted values until the desired prediction horizon is reached. The average root-mean-squared error (RMSE) of the predicted values are given in Tables V,VI, and VII for the three prediction horizons. It can be seen that the accuracy of prediction improved significantly and consistently across the range of prediction horizons and techniques for the CMA filtered time series compared to the unfiltered irregular signal. It proves that the self-similarity enhancement was effective regardless

TABLE V
RMSE OF PREDICTED VALUES IN VARIOUS FORECASTING METHODS: 1-MINUTE AHEAD

Prediction Method	I_t	$\hat{I}_t + \delta P_c$			
		ω_1	ω_2	ω_3	ω_4
Naïve, kW	413.7	195.4 (465.7)	163.0 (433.2)	138.9 (402.5)	120.9 (372.9)
Random Walk, kW	158.6	3.0 (5.3)	2.3 (4.7)	1.9 (4.3)	1.6 (4.0)
Markov Chain, kW	159.6	8.8 (20.3)	7.7 (19.7)	7.1 (19.1)	6.5 (18.4)
ANN, kW	166.3	1.1 (1.25)	0.8 (1.0)	0.6 (0.8)	0.5 (0.7)

$\omega_1 = 216$ min.; $\omega_2 = 288$ min.; $\omega_3 = 360$ min.; $\omega_4 = 432$ min.

TABLE VI
RMSE OF PREDICTED VALUES IN VARIOUS FORECASTING METHODS: 5-MINUTE AHEAD

Prediction Method	I_t	$\hat{I}_t + \delta P_c$			
		ω_1	ω_2	ω_3	ω_4
Naïve, kW	420.4	199.4 (475.1)	166.3 (442.0)	141.7 (410.6)	123.4 (380.4)
Random Walk, kW	352.9	14.2 (26.1)	11.1 (23.4)	9.2 (21.4)	7.8 (19.7)
Markov Chain, kW	353.5	16.4 (32.7)	13.3 (30.4)	11.5 (28.4)	10.1 (26.6)
ANN, kW	337.2	7.5 (30.6)	5.6 (9.3)	4.6 (6.6)	3.8 (6.3)

TABLE VII
RMSE OF PREDICTED VALUES IN VARIOUS FORECASTING METHODS: 60-MINUTE AHEAD

Prediction Method	I_t	$\hat{I}_t + \delta P_c$			
		ω_1	ω_2	ω_3	ω_4
Naïve, kW	476.6	257.9 (621.0)	216.1 (578.5)	184.5 (537.9)	160.8 (498.6)
Random Walk, kW	501.3	137.4 (295.1)	110.3 (270.4)	92.5 (249.4)	79.8 (230.1)
Markov Chain, kW	501.3	137.4 (295.6)	110.5 (271.1)	92.8 (250.1)	80.1 (230.7)
ANN, kW	617.0	130.0 (151.3)	102.3 (126.9)	91.3 (116.4)	65.7 (111.3)

of the forecasting technique and prediction horizon. It can also be observed that the prediction accuracy consistently improved from smaller ω values to the larger ones, which also correlates with the associated Hurst exponent in Table II. For 1-step ahead prediction horizon in Table V, the RMSE of prediction for the unfiltered irregular component, i.e., I_t, is 2.1∼3.4, 53∼99, 18∼24, and 151∼333 times worse than the prediction accuracy of the filtered time series using *naïve*, *random-walk*, *Markov Chain*, and *ANN* methods, respectively. The same observations can be made for 5- and 60-minute prediction horizons in Tables V-VII. The values in parentheses are the RMSE of predicted values for the filtered original time series, i.e., z_t, which is 1.6∼4.1 times worse than the prediction accuracy of the filtered decomposed signal using three forecast techniques. It proves that the seasonal decomposition has a significant impact on the outcome of filtering as a mechanism to enhance predictability. The magnitude of improvement is so significant that could justify the cost of the battery, as will be discovered in the next section. Moreover, significant improvement in prediction accuracy substantially reduces risks for the renewable generators to bid in the market more aggressively and gain more profit.

F. Economic Viability Assessment

A standard economic viability analysis is carried out to show the economic benefit of the battery application. The levelised cost of energy (LCOE) of the battery is estimated based on the battery kW/kWh size and rated energy throughput over the battery lifetime. The use of LCOE is standard and represents the price needed to cover operational and capital costs of the project while also earning an economic return. The total capital cost of the battery is calculated by:

$$\pi^{\omega_i} = E^{\omega_i} \times \pi_{\text{kWh}} + \mathbf{P}_{\omega_i}^{\mathbf{max}} \times \pi_{\text{kW}} \tag{10}$$

where π_{kWh} and π_{kW} are the unit cost of the battery energy and power capacity, respectively. The MWh throughput of the battery before reaching the EOL, i.e., $\mathcal{C}_{\text{total}}^{\omega_i}$, at nominal DoD can be obtained by Eq. (7b) for each battery size, i.e., E^{ω_i}, considering battery capacity degradation over its useful lifetime. The LCOE can then be estimated by:

$$\text{LCOE}^{\omega_i} = \frac{\pi^{\omega_i}}{\mathcal{C}_{\text{total}}^{\omega_i}} \tag{11}$$

Battery prices declined considerably in the last couple of years. As reported in [46], π_{kWh} and π_{kW} were about US$240/kWh and US$686/kW on average in 2016, respectively. The projection of the Bloomberg Energy was for the price to go down to π_{kWh} =US$162/kWh by the end of 2017. Rated battery cycle is quite different from one model of Li-Ion to another. As an example, the LG® Chem RESU battery is claimed to bear more than 6000 cycles at 90% DoD [47]. For Tesla Powerwall 2, this number is estimated at 7000 if the battery is operated at 100% DoD and no more than 14 kWh per day energy throughput (rated capacity is 3.3kW/13.5kWh) [48], [49]. In order to account for the uncertainty in price and rated cycle life of the battery, four different scenarios are defined for LCOE calculation, as follows:

- ◇ **scenario I**: $\text{DoD}_r = 0.9$, $\text{N}_r = 6000$, $\pi_{\text{kWh}} = 240$, and $\pi_{\text{kW}} = 686$
- ◇ **scenario II**: $\text{DoD}_r = 1.0$, $\text{N}_r = 7000$, $\pi_{\text{kWh}} = 240$, and $\pi_{\text{kW}} = 686$
- ◇ **scenario III**: $\text{DoD}_r = 0.9$, $\text{N}_r = 6000$, $\pi_{\text{kWh}} = 162$, and $\pi_{\text{kW}} = 686$
- ◇ **scenario IV**: $\text{DoD}_r = 1.0$, $\text{N}_r = 7000$, $\pi_{\text{kWh}} = 162$, and $\pi_{\text{kW}} = 686$

The LCOE values in different scenarios for various CMA filters are shown in Fig. 6 along with the average imbalance prices in four different markets, i.e., Australian energy market operator (AEMO), NordPool in Europe, California ISO (CAISO) and PJM in the USA, which were US$45.0/MWh (exchange rate AU$1=US$0.77) in AEMO in 2017 [50], US$36.6/MWh (exchange rate €1=US$1.23) NordPool [51], US$30/MWh in CAISO in 2015 [52], and US$16.1/MWh in PJM in 2017 [53].

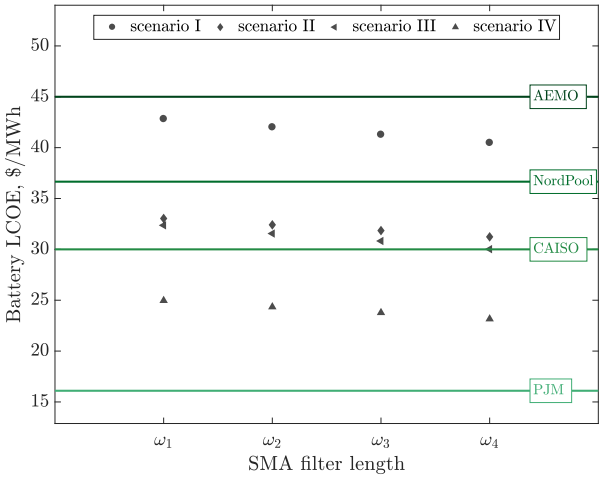

Fig. 6. LCOE of Li-Ion battery compared to the average regulation prices in different imbalance markets

It can be seen in Fig. 6 that the economic viability of the battery varies from one market to another. While all battery sizes in different scenarios make economic sense in AEMO, none of the scenarios is economically viable in the PJM imbalance market. Bear in mind that the opportunity loss due to conservative bidding is neglected in this analysis, which can further improve the economic viability of the battery in this application. With the current trend in Li-Ion cost reduction [46] and ever-increasing share of renewable in the electricity generation portfolio, which might increase regulation prices [54], higher economic advantage of the Li-Ion technology can be expected in the near future.

IV. Conclusion

In this study, an optimal battery sizing procedure is proposed based on the concept of predictability of a time series. The proposed procedure employs ACF for seasonality verification, STL for seasonal decomposition, ADF and KPSS tests to check on the stationarity of the irregular stochastic component, and an optimisation formulation to find optimal size of the battery based on the CMA filter. Hurst exponent estimation is used to quantify the predictability of the time series. Simulation results show that the given PV generation profile

has strong seasonality, which can be effectively removed for the sake of self-similarity studies. In addition, it is shown that larger battery sizes lead to higher Hurst exponent values, which essentially results in better predictability of the time series. It is verified by predicting minute-by-minute test dataset of 88 days using four different forecasting techniques and three prediction horizons. From the prediction simulation results, it is clear that the predictability is improved across different prediction techniques and time horizons. In addition, the economic viability analysis shows economic incentives to use battery in such application to avoid paying for the imbalance services. Also, there is a trade-off between the cost of battery and the benefit achieved by improving predictability of the PV production, which has not been considered in the problem formulation. The authors are currently working on developing an optimisation formulation by integrating the cost and benefit of battery, which requires finding a relationship between Hurst exponent and actual prediction improvement, and will be reported in our future works.

ACKNOWLEDGMENT

This work was performed in part using equipment and infrastructure funded by the Australian Federal Governments Department of Education, AGL Solar PV Education Investment Fund Research Infrastructure Project. The University of Queensland is the Lead Research Organisation in partnership with AGL, First Solar and the University of New South Wales.

REFERENCES

[1] P. Pinson, G. Papaefthymiou, B. Klockl, and J. Verboomen, "Dynamic sizing of energy storage for hedging wind power forecast uncertainty," in *Power & Energy Society General Meeting, 2009. PES'09. IEEE*. IEEE, 2009, pp. 1–8.

[2] H. Bludszuweit and J. A. Domínguez-Navarro, "A probabilistic method for energy storage sizing based on wind power forecast uncertainty," *IEEE Transactions on Power Systems*, vol. 26, no. 3, pp. 1651–1658, 2011.

[3] Y. Zheng, Z. Y. Dong, F. J. Luo, K. Meng, J. Qiu, and K. P. Wong, "Optimal allocation of energy storage system for risk mitigation of DISCOs with high renewable penetrations," *IEEE Transactions on Power Systems*, vol. 29, no. 1, pp. 212–220, 2014.

[4] C. Jaworsky, K. Turitsyn, and S. Backhaus, "The effect of forecasting accuracy on the sizing of energy storage," in *ASME 2014 Dynamic Systems and Control Conference*. American Society of Mechanical Engineers, 2014, pp. V002T22A005–V002T22A005.

[5] P. Haessig, B. Multon, H. B. Ahmed, S. Lascaud, and P. Bondon, "Energy storage sizing for wind power: impact of the autocorrelation of day-ahead forecast errors," *Wind Energy*, vol. 18, no. 1, pp. 43–57, 2015.

[6] F. Luo, K. Meng, Z. Y. Dong, Y. Zheng, Y. Chen, and K. P. Wong, "Coordinated operational planning for wind farm with battery energy storage system," *IEEE Transactions on Sustainable Energy*, vol. 6, no. 1, pp. 253–262, 2015.

[7] Q. Li, R. Ayyanar, and V. Vittal, "Convex optimization for DES planning and operation in radial distribution systems with high penetration of photovoltaic resources," *IEEE Transactions on Sustainable Energy*, vol. 7, no. 3, pp. 985–995, 2016.

[8] Y. Liu, W. Du, L. Xiao, H. Wang, S. Bu, and J. Cao, "Sizing a hybrid energy storage system for maintaining power balance of an isolated system with high penetration of wind generation," *IEEE Transactions on Power Systems*, vol. 31, no. 4, pp. 3267–3275, 2016.

[9] M. Brenna, F. Foiadelli, M. Longo, and D. Zaninelli, "Energy storage control for dispatching photovoltaic power," *IEEE Transactions on Smart Grid*, 2016.

[10] K. Baker, G. Hug, and X. Li, "Energy storage sizing taking into account forecast uncertainties and receding horizon operation," *IEEE Transactions on Sustainable Energy*, vol. 8, no. 1, pp. 331–340, 2017.

[11] P. Pflaum, M. Alamir, and M. Y. Lamoudi, "Battery sizing for PV power plants under regulations using randomized algorithms," *Renewable Energy*, vol. 113, pp. 596–607, 2017.

[12] C.-L. Nguyen and H.-H. Lee, "Power management approach to minimize battery capacity in wind energy conversion systems," *IEEE Transactions on Industry Applications*, vol. 53, no. 5, pp. 4843–4854, 2017.

[13] S. Majumder, S. A. Khaparde, A. P. Agalgaonkar, P. Ciufo, S. Perera, and S. V. Kulkarni, "Dft-based sizing of battery storage devices to determine day-ahead minimum variability injection dispatch with renewable energy resources," *IEEE Transactions on Smart Grid*, pp. 1–1, 2017.

[14] H. Nazaripouya, C. C. Chu, H. R. Pota, and R. Gadh, "Battery energy storage system control for intermittency smoothing using an optimized two-stage filter," *IEEE Transactions on Sustainable Energy*, vol. 9, no. 2, pp. 664–675, April 2018.

[15] F. Zhang, G. Wang, K. Meng, J. Zhao, Z. Xu, Z. Y. Dong, and J. Liang, "Improved cycle control and sizing scheme for wind energy storage system based on multiobjective optimization," *IEEE Transactions on Sustainable Energy*, vol. 8, no. 3, pp. 966–977, 2017.

[16] F. Zhang, K. Meng, Z. Xu, Z. Dong, L. Zhang, C. Wan, and J. Liang, "Battery ESS planning for wind smoothing via variable-interval reference modulation and self-adaptive SOC control strategy," *IEEE Transactions on Sustainable Energy*, vol. 8, no. 2, pp. 695–707, 2017.

[17] J. Garland, R. James, and E. Bradley, "Model-free quantification of time-series predictability," *Physical Review E*, vol. 90, no. 5, p. 052910, 2014.

[18] Y. Yang, S. Bremner, C. Menictas, and M. Kay, "Battery energy storage system size determination in renewable energy systems: A review," *Renewable and Sustainable Energy Reviews*, vol. 91, pp. 109–125, 2018.

[19] R. B. Cleveland, W. S. Cleveland, and I. Terpenning, "STL: A seasonal-trend decomposition procedure based on Loess," *Journal of Official Statistics*, vol. 6, no. 1, p. 3, 1990.

[20] G. Samorodnitsky, "Long memory and self-similar processes," in *ANNALES-FACULTE DES SCIENCES TOULOUSE MATHEMATIQUES*, vol. 15, no. 1. Université Paul Sabatier, 2006, p. 107.

[21] J. A. Matos, S. M. Gama, H. J. Ruskin, A. Al Sharkasi, and M. Crane, "Time and scale hurst exponent analysis for financial markets," *Physica A: Statistical Mechanics and its Applications*, vol. 387, no. 15, pp. 3910–3915, 2008.

[22] L. Das, B. Srinivasan, and R. Rengaswamy, "Multivariate control loop performance assessment with hurst exponent and mahalanobis distance," *IEEE Transactions on Control Systems Technology*, vol. 24, no. 3, pp. 1067–1074, 2016.

[23] J. Shen, S. Dusmez, and A. Khaligh, "Optimization of sizing and battery cycle life in battery/ultracapacitor hybrid energy storage systems for electric vehicle applications," *IEEE Transactions on industrial informatics*, vol. 10, no. 4, pp. 2112–2121, 2014.

[24] J. Song, V. Krishnamurthy, A. Kwasinski, and R. Sharma, "Development of a markov-chain-based energy storage model for power supply availability assessment of photovoltaic generation plants," *IEEE Transactions on Sustainable Energy*, vol. 4, no. 2, pp. 491–500, 2013.

[25] M. Q. Raza, M. Nadarajah, and C. Ekanayake, "On recent advances in PV output power forecast," *Solar Energy*, vol. 136, pp. 125–144, 2016.

[26] M. P. Almeida, M. Muñoz, I. de la Parra, and O. Perpiñán, "Comparative study of PV power forecast using parametric and nonparametric PV models," *Solar Energy*, vol. 155, pp. 854–866, 2017.

[27] J. Beran, Y. Feng, S. Ghosh, and R. Kulik, *Long-memory processes probabilistic: Properties and statistical methods*. Springer, 2013, vol. 884.

[28] N. Korolko, Z. Sahinoglu, and D. Nikovski, "Modeling and forecasting self-similar power load due to EV fast chargers," *IEEE Transactions on Smart Grid*, vol. 7, no. 3, pp. 1620–1629, 2016.

[29] M. Natrella, "NIST/SEMATECH e-handbook of statistical methods," http://www.itl.nist.gov/div898/handbook/pmc/section4/pmc443.htm, 2010, accessed: 2017-12-05.

[30] G. E. Box, G. M. Jenkins, G. C. Reinsel, and G. M. Ljung, *Time series analysis: forecasting and control*. John Wiley & Sons, 2015.

[31] R. J. Hyndman and G. Athanasopoulos, *Forecasting: principles and practice*. OTexts, 2014.

[32] R. Weron, *Modeling and forecasting electricity loads and prices: A statistical approach*. John Wiley & Sons, 2007, vol. 403.

[33] W. A. Fuller, *Introduction to statistical time series*. John Wiley & Sons, 2009, vol. 428.

[34] D. Kwiatkowski, P. C. Phillips, P. Schmidt, and Y. Shin, "Testing the null hypothesis of stationarity against the alternative of a unit root: How sure are we that economic time series have a unit root?" *Journal of econometrics*, vol. 54, no. 1-3, pp. 159–178, 1992.

[35] M. S. Taqqu, V. Teverovsky, and W. Willinger, "Estimators for long-range dependence: an empirical study," *Fractals*, vol. 3, no. 04, pp. 785–798, 1995.
[36] S. Orfanidis, *Introduction to signal processing*. Pearson Education, 2010.
[37] P. J. Brockwell and R. A. Davis, *Introduction to time series and forecasting*. springer, 2016.
[38] F. Geth, J. Tant, D. Six, P. Tant, T. De Rybel, and J. Driesen, "Techno-economical and life expectancy modeling of battery energy storage systems," in *Proceedings of the 21st International Conference on Electricity Distribution (CIRED)*, 2011.
[39] A. Sinha, P. Malo, and K. Deb, "Tutorial on bilevel optimization," 2013. [Online]. Available: https://wiki.aalto.fi/display/~ansinha@aalto.fi/Tutorial+on+Bilevel+Optimization
[40] M. Alam, R. Yan, T. Saha, A. Chidurala, and D. Eghbal, "Learning from a 3.275 MW utility scale PV plant project," *CIGRé*, 2016.
[41] R. Yan, T. K. Saha, P. Meredith, A. Ananth, and M. I. Hossain, "Megawatt-scale solar variability study: an experience from a 1.2 MWp photovoltaic system in australia over three years," *IET Renewable Power Generation*, vol. 10, no. 8, pp. 1229–1236, 2016.
[42] I. Gurobi Optimization, "Gurobi optimizer reference manual," 2016. [Online]. Available: http://www.gurobi.com
[43] H.-x. Zhao and F. Magoulès, "A review on the prediction of building energy consumption," *Renewable and Sustainable Energy Reviews*, vol. 16, no. 6, pp. 3586–3592, 2012.
[44] S. P. Kani and M. Ardehali, "Very short-term wind speed prediction: a new artificial neural network–markov chain model," *Energy Conversion and Management*, vol. 52, no. 1, pp. 738–745, 2011.
[45] A. K. Yadav and S. Chandel, "Solar radiation prediction using artificial neural network techniques: A review," *Renewable and Sustainable Energy Reviews*, vol. 33, pp. 772–781, 2014.
[46] C. Curry, "Lithium-ion battery costs and market: Squeezed margins seek technology improvements and new business models," https://data.bloomberglp.com/bnef/sites/14/2017/07/BNEF-Lithium-ion-battery-costs-and-market.pdf, accessed: 2018-03-17.
[47] "LG Chem RESU: Li-Ion battery," http://batterytestcentre.com.au/results/lg-chem-resu/, accessed: 2018-03-17.
[48] "Tesla Powerwall 2," https://www.tesla.com/sites/default/files/pdfs/powerwall/Powerwall%202_AC_Datasheet_en_northamerica.pdf, accessed: 2018-03-17.
[49] "The Tesla Powerwall 2: Batteries can finally pay for themselves," https://www.solarquotes.com.au/blog/tesla-powerwall-2/, accessed: 2018-03-17.
[50] "Balancing market summary," http://data.wa.aemo.com.au/#balancing-summary, accessed: 2018-03-23.
[51] "NordPool: Historical market data," https://www.nordpoolspot.com/historical-market-data/, accessed: 2018-03-17.
[52] D. of Market Monitoring, "Q1 2016 report on market issues and performance," California ISO, Tech. Rep., Jun. 2016. [Online]. Available: http://www.caiso.com/Documents/2016FirstQuarterReportMarketIssuesandPerformance.pdf
[53] "PJM: Ancillary service market results," http://www.pjm.com/markets-and-operations/ancillary-services.aspx, accessed: 2018-03-24.
[54] A. Blakers, B. Lu, and M. Stocks, "100% renewable electricity in Australia," *Energy*, vol. 133, pp. 471–482, 2017.

Ali Pourmousavi Kani (S'07, M'15) received the B.Sc., M.Sc., and PhD degrees with honours in 2005, 2008, and 2014, respectively, in electrical engineering. He worked for California ISO, NEC Laboratories America Inc., and Denmark Technical University (DTU) from 2014 to 2017. He is currently a research fellow at the University of Queensland (UQ), Australia. His current research interests include battery and its integration to the grid for different applications, control-based ancillary services, and demand response.

Phil Wild has a PhD from the University of Queensland, Brisbane, Australia in the field of Economics. He has expertise in time series analysis including knowledge of decomposition techniques, stationary and non-stationary processes, trend removal techniques (including unit roots), short and long memory (self-similar) processes and forecasting methodologies. His current research interests include wholesale electricity market modelling, integrating high penetrations of intermittent renewables, yield analysis of variable renewables and financial viability analysis.

Tapan Kumar Saha (M'93, SM'97) was born in Bangladesh in 1959 and immigrated to Australia in 1989. He received his B. Sc. Engineering (Electrical and Electronic) in 1982 from the Bangladesh University of Engineering & Technology, Dhaka, Bangladesh, M. Tech (Electrical Engineering) in1985 from the Indian Institute of Technology, New Delhi, India and PhD in 1994 from the University of Queensland, Brisbane, Australia. Tapan is currently a Professor of Electrical Engineering in the School of Information Technology and Electrical Engineering, University of Queensland, Australia. He is a Fellow of the Institution of Engineers, Australia. His research interests include condition monitoring of electrical assets, power systems and power quality.